Recent Advances in Thermal Imaging and Its Applications Using Machine Learning: A Review

A. N. Wilson, Khushi Anil Gupta, Balu Harshavardan Koduru, Abhinav Kumar, *Senior Member, IEEE*, Ajit Jha, and Linga Reddy Cenkeramaddi, *Senior Member, IEEE*

***Abstract*—Recent advancements in thermal imaging sensor technology have resulted in the use of thermal cameras in a variety of applications, including automotive, industrial, medical, defense and space, agriculture, and other related fields. Thermal imaging, unlike RGB imaging, does not rely on background light, and the technique is nonintrusive while also protecting privacy. This review article focuses on the most recent advancements in thermal imaging technology, key performance parameters, an overview of its applications, and machine-learning techniques applied to thermal images for various tasks. This article begins with the most recent advancements in thermal imaging, followed by a classification of thermal cameras and their key specifications, and finally a review of machine-learning techniques used on thermal images for various applications. This detailed review article is highly useful for designing thermal imaging-based applications using various machine-learning techniques.**

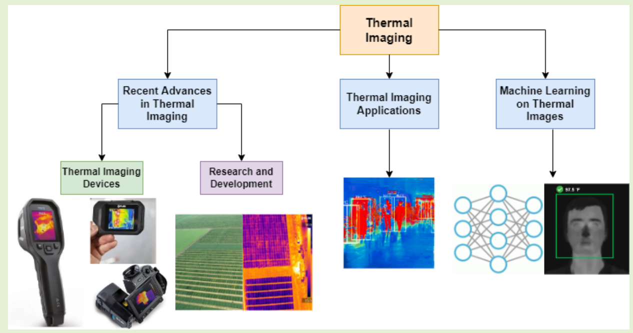

***Index Terms*—Agriculture applications, automotive applications, computer vision, industrial applications, machine learning, medical applications, space and defense applications, thermal camera, thermal imaging, thermal imaging applications.**

I. Introduction

Since 1960, thermal imaging was confined only to military [1] and medical [2] applications, however, with the recent advancements in chip technology and lower cost, thermal imaging has gained widespread popularity. Thermal imaging works by utilizing the radiation in the infrared region of the spectrum, specifically the wavelengths from 3 to 14 μm. These wavelengths are subdivided into different subbands as shown in Table I. Special devices called thermal imagers utilize the infrared part of the spectrum to obtain a spatial temperature distribution map of the captured scene [3]. Each pixel in the temperature map depicts the relative temperature of that point in the environment. These temperature maps can be easily used for real-time applications with proper calibration, bias removal, and further processing [4].

Thermal imaging technology is independent of any external light source because it is based solely on the detection of infrared radiations (IRs) emitted by objects. As a result, the technology is found to have a faster processing speed than its RGB counterparts [5]. Thermal imaging devices are now being widely used in civilian applications such as fever scanners, insulation detectors, and electrical hotspot detectors due to lower chip costs, improved portability, and flexible designs. Combining thermal cameras with RGB cameras has also gained popularity due to their ability to complement

TABLE I
Subbands in the Infrared Spectrum

S No.	IR Band	Wavelength (in nm)
1	Near infrared	700 – 1400
2	Short range wavelength infrared	1400 – 3000
3	Mid range wavelength infrared	3000 – 8000
4	Long range wavelength infrared	8000 – 15000
5	Far infrared	15000 – 1000000

Manuscript received 10 November 2022; accepted 1 January 2023. Date of publication 10 January 2023; date of current version 13 February 2023. This work was supported in part by the INTPART Program from the Research Council of Norway through the Indo-Norwegian Collaboration in Autonomous Cyber-Physical Systems (INCAPS) Project under Grant 287918 and in part by the Low-Altitude UAV Communication and Tracking (LUCAT) through the IKTPLUSS Program from the Research Council of Norway under Project 280835. The associate editor coordinating the review of this article and approving it for publication was Prof. Pai-Yen Chen. *(Corresponding author: Linga Reddy Cenkeramaddi.)*

A. N. Wilson and Linga Reddy Cenkeramaddi are with the ACPS Group, Department of Information and Communication Technology, University of Agder, 4879 Grimstad, Norway (e-mail: wilson.a.nelson@uia.no; linga.cenkeramaddi@uia.no).

Khushi Anil Gupta was with the ACPS Group, Department of Information and Communication Technology, University of Agder, 4879 Grimstad, Norway. She is now with the Department of Electrical Engineering, Columbia University, New York, NY 10027 USA (e-mail: kg3023@columbia.edu).

Balu Harshavardan Koduru was with the ACPS Group, Department of Information and Communication Technology, University of Agder, 4879 Grimstad, Norway. He is now with the Institute for Artificial Intelligence and Data Science, University of Buffalo, Buffalo, NY 14260 USA (e-mail: baluhars@buffalo.edu).

Abhinav Kumar is with the Department of Electrical Engineering, Indian Institute of Technology Hyderabad, Hyderabad 502285, India (e-mail: abhinavkumar@ee.iith.ac.in).

Ajit Jha is with the Department of Engineering Science, University of Agder, 4879 Grimstad, Norway (e-mail: ajit.jha@uia.no).

Digital Object Identifier 10.1109/JSEN.2023.3234335

TABLE II
COMPARISON OF PREVIOUS REVIEW ARTICLES WITH OUR WORK

Year	Reference	Focus areas	RA	Appl.	CM	Image Pro.	ML Tech.	Comments
2005	[8]	Image processing techniques for active and passive thermography	✗	✗	✗	✓	✗	Restricted to processing techniques
2009	[9]	Status of intra-operative thermal imaging and case report on it's advantages and applications	✓	✓	✗	✗	✗	Restricted to intra-operative thermal imaging
2014	[10]	Uses and applications of thermal Imaging in Agriculture	✓	✓	✗	✗	✗	Restricted to the field of agriculture
2017	[11]	Theory behind thermal imaging and its applications in different fields	✓	✓	✗	✗	✗	Restricted to working and applications of thermal imaging
2020	[12]	Techniques for face Emotion detection using thermal imaging	✓	✓	✗	✗	✓	Restricted to facial emotion detection
2020	[13]	Review of techniques and methodologies on diagnosing breast cancer using thermal imaging	✓	✓	✓	✗	✗	Restricted to applications in breast cancer diagnosis
2021	[14]	Role of thermal sensors and imaging in aerial navigation systems	✓	✓	✓	✗	✓	Restricted to aerial navigation systems
2022	**Our Work**	**Recent advancements in thermal imaging, latest models of thermal cameras available in the market, image processing and machine learning techniques related to thermal imaging**	✓	✓	✓	✓	✓	**Not restricted to particular filed of study or application**

RA - Recent Advancements; **Appl.** - Applications; **CM** - Current Models in market; **Image Pro.** - Image Processing; **ML Tech.** - Machine Learning Techniques

each other's features [4]. In addition to the benefits listed above, thermal imaging provides a noncontact, noninvasive method known as infrared thermography for obtaining useful information about a patient's health and diagnosis, which has widespread medical applications [6].

The high sensitivity of thermal cameras has enabled them to be used in optical applications as well [7]. Other applications enabled by thermal imaging include fire prediction, weather forecasting, and animal monitoring [7]. RGB cameras depend on illumination and reflection from the objects, whereas thermal cameras are sensitive to the emitted IR, even if the object is cold [7]. Because each object's heat signature is unique, thermal cameras have an advantage over standard RGB cameras in distinguishing between similar objects.

Thermal cameras have grown in popularity and use as a result of the benefits listed above. This article focuses on various key technological advancements to provide a glimpse into the most recent developments in this technology. This article primarily highlights the various types of thermal imaging devices/cameras on the market, thermal camera selection criteria based on application and specifications, recent machine-learning techniques for thermal image processing, and potential future research directions. Our survey article differs from others in terms of application focus, recent advancements, a brief overview of camera models, and machine-learning techniques. Table II highlights the most important aspects of this article, demonstrating how it differs from previous surveys.

The remainder of this article is structured as follows. Section III focuses on recent advancements in thermal imaging that includes different thermal camera models and the latest research and development in the area. Section IV presents different thermal imaging-based applications. Section V goes over the recent machine-learning techniques used along with thermal imaging. Finally, Section VI concludes this article.

II. PRINCIPLE OF THERMAL SENSING

Thermal imaging is a noncontact and nondestructive method to measure the temperature of an object [15]. Thermal imaging utilizes the IR emitted from an object to create a visual temperature profile of the captured scene. As shown in Table I, the infrared spectrum is divided into different subbands based on their wavelength. The wavelength determines the intensity of IR that is emitted. Thermal imaging technology utilizes this energy intensity to generate the temperature map of the captured scene. The amount of thermal radiation emitted by a body primarily depends on the temperature (T) of the body and its emissivity factor (ε). The emissivity factor represents the ratio of energy emitted from a body to that of a perfect blackbody at the same temperature. The emissivity factor is 1 for a perfect blackbody and 0 for a perfect white body. Based on the IR energy radiated from a body, the surface temperature T_s of the body can be calculated as follows:

$$W = \left[\frac{2\pi^5 k^4}{15c^2h^3}\right] T^4 = \sigma T_s^4 \tag{1}$$

where W represents the energy flux emitted per unit area ($\mathrm{Wm^{-2}}$) of the body, c is the speed of light in vacuum (3×10^8 $\mathrm{ms^{-1}}$), k is Boltzmann's constant (1.38×10^{-23} $\mathrm{JK^{-1}}$), σ is Stefan–Boltzmann's constant (5.67×10^{-8} $\mathrm{Wm^{-2}K^{-4}}$), h is Planck's constant (6.63×10^{-34} Js), and T is the temperature of the body in Kelvin.

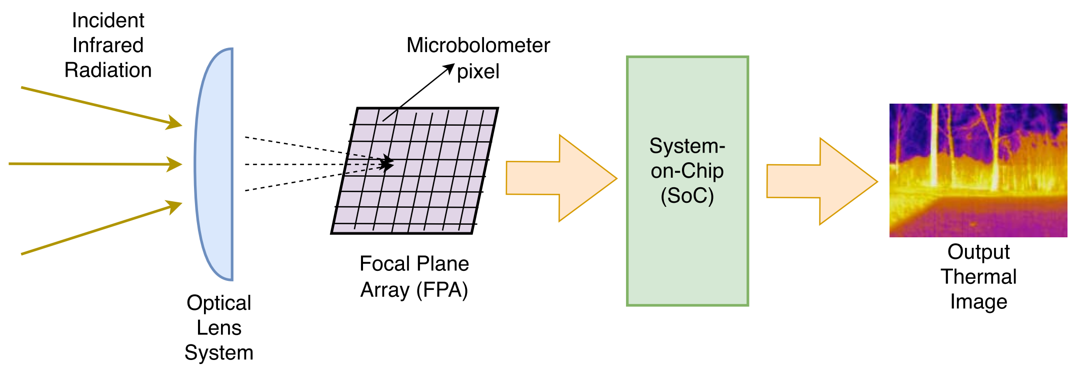

Fig. 1. Working of the bolometer-based thermal sensor.

TABLE III
POPULAR THERMAL SENSORS AND KEY SENSING TECHNOLOGY

Sl. No.	Model	Type	Material	Manufacturer
1	Lepton 3.5 [19]	Bolometer	Vanadium-oxide (VOx)	FLIR
2	Pyrosens [20]	Pyroelectric	Lithium tantalate	DIAS Infrared
3	InspectionCAM IQ-AAA [21]	Bolometer	Vanadium-oxide (VOx)	Seek Thermal
4	D6T [18]	MEMS-based thermoelectric	-	Omron
5	Evo Thermal 90 [22]	Thermoelectric	-	Terabee

When (1) is applied to real objects, then the surface temperature is computed as

$$W = \varepsilon \sigma T^4 \tag{2}$$

where ε is the object's emissivity. By utilizing W, we can obtain a thermal visualization of the captured scene which is the basis of thermal imaging [15].

The primary component of a thermal imaging system is the thermal detector/sensor. The thermal detector is responsible for mapping the incident IR to an appropriate temperature value. Based on the operating principle, thermal detectors are classified into three types: pyroelectric, thermoelectric, and bolometer sensors as shown in Table III. Pyroelectric sensors are made up of special materials that accumulate the charge on the basis of incident IR. A temperature change in the captured scene induces a proportional change in the accumulated charge. This change in the accumulated charge is used to obtain the thermal profile of the scene [16]. On the other hand, thermoelectric sensors operate according to the Seebeck effect [17]. Seebeck effect is the phenomenon by which a voltage difference is produced based on the temperature difference between two dissimilar electrical conductors. Microelectromechanical systems (MEMS)-based thermoelectric sensors focus the incident IR onto a thermoelectric sensor. The amount of incident IR generates an equivalent voltage. The induced voltage is then used to compute the object's temperature using interpolation and lookup table approximations [18]. Compared to pyroelectric sensors, thermoelectric sensors are reliable and cheap. However, thermoelectric sensors suffer from nonlinearity issues due to the nonlinear dependence between the output voltage and measured temperature.

Recently, bolometer-based thermal detectors have gained popularity due to their high thermal sensitivity, small size, and high accuracy. A bolometer is a special material whose electrical resistance responds to the amount of IR incident on it. Commonly used materials for bolometers include vanadium oxide (VOx) and amorphous silicon (a-Si). An example of a bolometer-based thermal sensor is the FLIR Lepton 3.5 [19]. The FLIR Lepton 3.5 uses a VOx-based microbolometer array for thermal imaging. Fig. 1 shows a simplified block diagram of the operation of a microbolometer-based thermal sensor. Fig. 1 shows that the optical lens system focuses the incident IR onto the focal plane array (FPA). Each element on the FPA represents a pixel and each pixel is in turn a VOx microbolometer that responds to the incident flux by producing a temperature change. The temperature change is proportional to the resistance of the microbolometer. The change in resistance is captured by the voltage fluctuations, which is fed into a system-on-chip (SoC). The SoC performs the necessary signal processing and outputs the thermal profile of the scene [19].

III. RECENT ADVANCES IN THERMAL IMAGING

The early thermal camera sensors were designed with a lens filled with gas. They also required refrigeration to function properly. However, due to advancements in semiconductor technology, thermal cameras are now comparable to standard charge-coupled device (CCD) cameras. Furthermore, their improved portability and low cost have made them suitable for use in several applications [23].

Advancements in thermal imaging have paved way for thermal camera sensors that can help in enhancing user interaction with the environment. Thermal imaging-based sensors are used in games to identify the effect of moral decisions based on the user's facial heat map [24]. Thermal cameras have become portable and easy to integrate such that they are now being used in pocket devices like FLIR C2, FLIR One, Cat S60, and Landguide M4 [4]. Recently, dual camera systems with a thermal camera integrated along with visual cameras have been developed to provide application-based

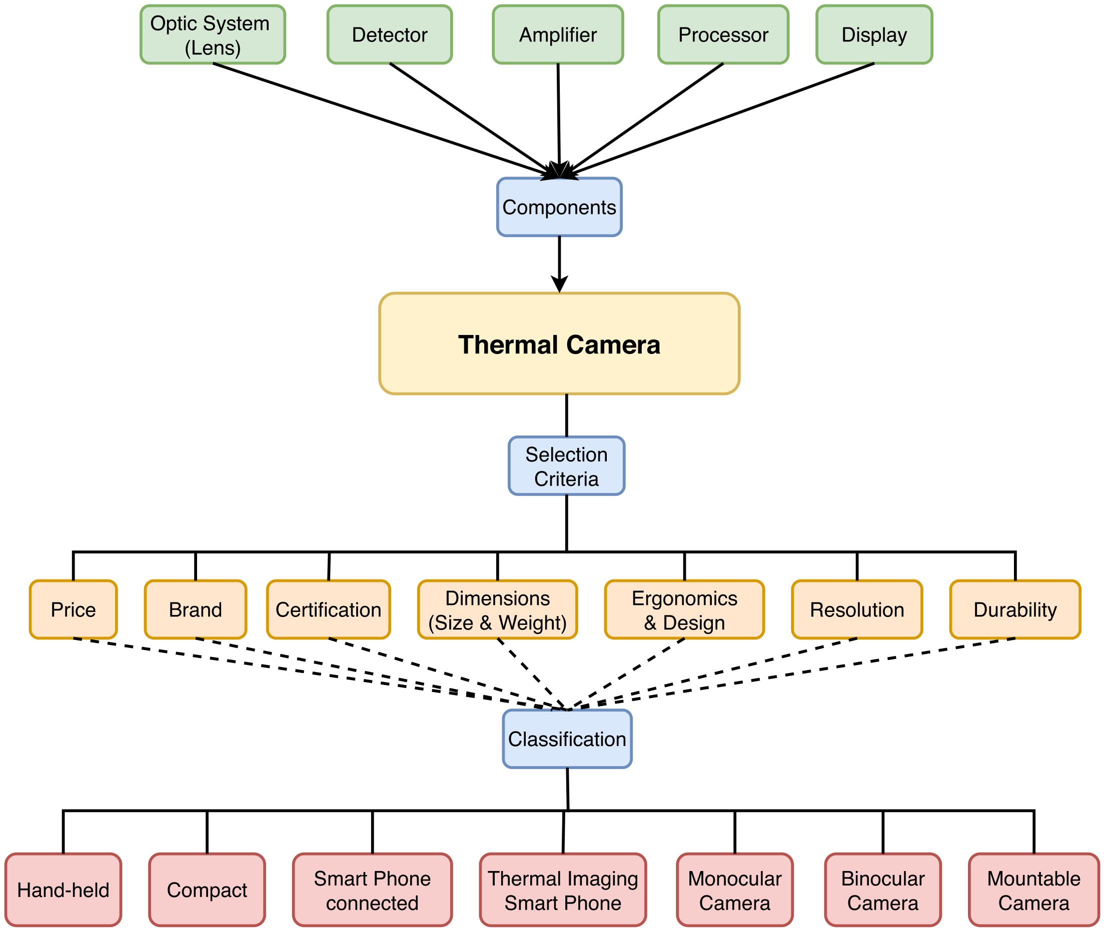

Fig. 2. Components, selection criteria, and classification of thermal cameras.

usage, that is, when surveillance is required, the thermal camera mode is enabled in the dual-camera setup. The dual-camera setup is used in parking lots to determine car parking history or recently occupied parking spots based on the heat emitted from the engines or surrounding surfaces [4]. However, thermal camera integration with a visual camera increases the bandwidth of applications. As thermal cameras cannot detect visual information such as numbers, signs, and words, integration of an optical image provides an additional advantage to the thermal image, thereby enhancing it [25]. Through this overlay of optical and thermal images, highly informative and contrast images are obtained, making the detection of hotspots and sources of fire and heat easier. Currently, thermal cameras have become ubiquitous with a wide variety of selections to choose from. Fig. 2 displays the various types of thermal camera classes. These are categorized with respect to factors such as usage, application, temperature, and range as explained in Table IV.

A. Latest Developments in Thermal Cameras

This section discusses the latest thermal camera models available in the market. Table V shows the different thermal camera models along with some key metrics, which can help in deciding the right thermal camera for different applications. Thermal camera models from companies FLIR and MOBOTIX have been discussed here along with their suitability in accordance with various applications.

FLIR thermal imaging cameras are used for predictive maintenance. They are also equally used by electricians and technicians to detect and resolve electrical issues, isolation issues, and so on. These cameras are well suited for making long-distance inspections with accurate temperature profiles [35]. Furthermore, the multispectral dynamic imaging (MSX) feature in these cameras enables MSX to make the thermal images more refined. The interfaces are also well developed to ensure easy transfer of output data. This feature can be found in Ex, Exx, and the T-series versions of FLIR thermal cameras [36].

The E-series thermal camera range includes E4, E5, E6, and E8, all of which are highly portable and can be used to detect hidden defects. This allows technicians to take an instant action in response to a situation before it becomes too serious [36]. These cameras have thermal, visible, and MSX imaging. Based on the type of E-series model, the IR imaging resolution can be adjusted; E4 (up to 4800 pixels), E5 (up to 10 800 pixels), E6 (up to 19 200 pixels), and E8 (up to 76 800 pixels). The E40, E50, and E60 models are for frequent and wide-angled inspection for onsite technicians and electricians. These cameras also have high wireless connectivity and touchscreen control to do an instant analysis of the captured thermal images [36]. FLIR T-series is suited

TABLE IV
SUITABLE CAMERA MODEL WITH RESPECT TO THE APPLICATIONS

S.No.	Temperature	Range	Inspection	Application	Model
1.	Low	Short	Quick and small	Facility maintenance, HVACs pros	E4 through E8
2.	High	Mid and short	Small	Electricians and plant site maintenance	E40 through E60
3.	Low and high	Mid, short, and long	Intensive	Substation surveys and solar farm surveys	T420 to T640

TABLE V
POPULAR THERMAL CAMERAS AND THEIR SPECIFICATIONS

Sl. No.	Model Name (Brand)	Camera Type	Size (mm)	Sensor Resolution (pixels)	Price (USD)	Detecting Temperature Range (°C)	Thermal Sensitivity (°C)	User Interface and Connectivity	References
1	FLIR C5 (Teledyne FLIR)	Compact Pocket Thermal Camera	138 x 84 x 24	160 x 120	855	$-20 - 400$	$0 - 100$: ± 3 ; $100 - 400$: $\pm 3\%$	Touchscreen; FLIR Ignite cloud connectivity (using Wi-Fi)	[26]
2	Ti480 PRO (Fluke)	Hand-held Camera	277 x 122 x 167	640 x 480	–	$-20 - 1000$	± 2 or 2%	Touch screen; Wireless connectivity (Smart Phone, PC); Fluke Connect® app compatible	[27]
3	CompactPRO XR (Seek Thermal)	Smart Phone Connected Thermal Camera	25.4 x 44.45 x 25.4	320 x 240	599	$-40 - 330$	< 0.070	Seek Thermal app	[28]
4	Helion 2 XP50 Pro (Pulsar)	Monocular Camera	242 x 75 x 60	640 x 480	4376	–	< 0.025	Built-in WiFi module - connects to Smart Phones using Stream Vision 2 app	[29]
5	CAT S62 PRO (CAT)	Thermal Imaging Smart Phone	158.5 x 76.7 x 11.9	1440 x 1080	530	$-20 - 400$	–	5.7” FHD + Display	[30]
6	Merger LRF XP50 (Pulsar)	Binocular Camera	196 x 143 x 76	640 x 480	6486	–	< 0.025	Built-in WiFi module - connects to Smart Phones using Stream Vision 2 app	[31]
7	RSE600 (Fluke)	Mountable Camera	83 x 83 x 165	640 x 480	–	$-10 - 1200$	± 2 or $\pm 2\%$	SmartView® desktop software	[32]
8	M16B Thermal TR (MOBOTIX)	Mountable Camera	210 x 158 x 207	336 x 252	–	$-40 - 170$	± 0.05	HD wideband audio, Ethernet, RS232 support	[33]
9	S16B DualFlex (MOBOTIX)	Mountable Camera	130 x 115 x 33	336 x 252	–	$-40 - 160$	± 0.05	HD wideband audio, Ethernet, RS232 support	[34]

for measurements in extreme conditions such as long-range or high temperatures. It has a rotating optical block and autorotation feature to correctly aim the target for exact measurement and a better view for analysis and capture. T620 and T640 have built-in GPS to add a location to the thermal image for better labeling [36]. FLIR A655sc can be used in applications where the thermal camera mount needs to be fixed. For InGaAs detection, FLIR A6200sc thermal camera is suitable. For high-speed mid-wave infrared (MWIR), the FLIR X8400sc series shows promise [36].

MOBOTIX thermal cameras are widely used for surveillance applications. M16 Thermal [37] has two adjacent lenses which do thermal overlay with the visual image to pinpoint the location of hotspots like fire-affected regions in an image. An M16 TR thermal camera [38] is a low-power camera that has an additional thermal radiometry feature that enables the measurement of thermal radiation in the image. S16 DualFlex is a flexible dual-thermal camera with one or two weatherproof sensors which can withstand any conditions due to the robust casing around the dual-camera sensor setup [25], [39]. S16 TR [40] enables the radiation values to trigger an alarm or activation to alert the user if the temperature values exceed or are lesser than the threshold values calibrated in the sensor. Choosing a thermal camera for a particular application requires careful consideration of a variety of factors as it is a long-term investment. One needs to keep in mind the right supplier to suit the needs, as the functioning of the thermal camera depends largely on its hardware. The different thermal camera selection criteria are as shown in Fig. 2.

To choose the right camera model based on the application, the following characteristics should be kept in mind [41].

1) *Camera resolution:* Based on the application, it can be decided if a basic resolution model is required or an advanced one is. The basic resolution is around

60 × 60 pixels. 320 × 240 pixels offer superior definition and for even more advanced resolution 640 × 480 is suitable.

2) *Thermal sensitivity:* Thermal sensitivity indicates the thermal camera's ability to sense minute variations in temperature. The higher the value of sensitivity, the more accurately the camera can measure lower temperature differences. Hence, in industrial applications where such conditions of lower temperature differences prevail, a thermal camera with high-temperature sensitivity should be selected.
3) *Accuracy:* Depending upon the desired accuracy of the temperature readings, a suitable thermal camera model should be selected. Currently, the standard accuracy values are ±2% or ±2 °C. However, in more advanced thermal cameras, the accuracy ranges as ±1% or ±1 °C.
4) *Camera features:* Based on the application, having the right set of features for the thermal camera is necessary to ensure smooth operations. In certain applications, a dual-camera setup of the visual and thermal camera is required. In others, thermal fusion must be a necessity. In-built GPS helps to determine the location which can be useful in unmanned aerial vehicle (UAV) applications, whereas, in others, portability is the prime feature. Thus, it can be seen that according to the preference of various camera features, a suitable thermal camera model should be selected.
5) *Software:* Software compatibility with the corresponding hardware is essential to maintain operations. Hence, based on the intense level of inspection, the corresponding software should be selected.

The following are the most important considerations to make when selecting a particular thermal camera [41].

1) *Hardware:* It is advantageous to have a wide range of hardware to meet the needs of any custom application at all stages of development, from basic inspection equipment to advanced high-resolution-defined thermal image-producing cameras.
2) *Software:* The software should be compatible with the application and hardware platform, as the software defines how the image will be produced and displayed. Hence, based on the information that should be retrieved from the image, appropriate software should be chosen.
3) *Hardware interfaces:* It is ideal to have multiple hardware interfaces such as I2C, SPI, and USB so that they can be used with a variety of hard platforms and embedded/edge devices.

B. Future Work in Thermal Imaging

Due to the vast scope of thermal imaging and its utilization in different applications, most of the research in thermal imaging is in the production of sophisticated thermal cameras. These cameras are more application-specific and have greater range, sensitivity, and tolerance. Interestingly, thermal imaging is being used in a variety of new applications [42]. Researchers use thermal imaging to detect anxiety and classify it based on the heat map of the face. As stated in medical research, based on the type of anxiety, the bloodflow in the face can get altered. Certain types of anxiety can trigger more bloodflow in the cheeks, whereas others can incite low bloodflow in the forehead [23]. Current research is also focused on Airborne thermography in which high-resolution thermal imaging is used to measure crop fields on the basis of temperature, drought tolerance of crops, and efficient water delivery [42].

IV. Applications of Thermal Imaging

A vast majority of applications involve the use of thermal imagery as shown in Fig. 3. These include detecting cracks in building structures [48], identifying breast cancer [2], surveillance [44], autonomous driving [49], and so on. Thermal cameras are favored primarily because of their ability to obtain useful information in a noncontact nonintrusive manner. High-resolution thermal cameras are employed to detect temperature variations in different parts of the human body which can in turn help in medical diagnosis. The development of a neonatal in intensive care units can be assessed based on the time-dependent thermal variations obtained from thermal imaging. As the method is noncontact and noninvasive, it poses a reduced risk to neonatals [50]. Thermal imagery also helps to identify irregularities and detect diseases early. Breast cancer identification [51], [52], tumor detection [53], diabetic foot inspection [47], [54], COVID-19 screening [45], [55], diabetic eye disease [56], and skin cancer lesions [57] are some areas where thermal imaging has an edge over other traditional methods. Other applications include dental diagnosis where the number of deposits and activity on the tooth root caries are effectively measured using thermal imaging to make accurate decisions [58].

One of the earliest uses of thermal cameras stems from military and defense applications. Thermal cameras can easily identify intruders in the dark proving to be an effective sensing technology in low-light environments. Additionally, they aid in surveillance [44], detection and tracking of UAVs [59], ship navigation [36], flight landing assistance [60], maintaining border security [61], and so on.

Industrial applications for handheld thermal cameras have also gained prominence due to their ease to carry and detect faults and issues. Issues with electrical insulation [41], pipeline rework [46], and power-line inspection [46] are some areas where thermal cameras have helped improve industrial processes. Additionally, they are also used in welding applications to inspect defects [62]. Similarly, in civil and construction, thermal imagery helps to identify air leakages in buildings, defects, and cracks in bridge structures [48], etc.

Thermal cameras are used in agriculture for crop monitoring, yield forecasting, and irrigation scheduling [43]. Monitoring field nurseries to detect early diseases in tender seeds using thermal signatures has helped improve yield. In addition to the above applications, thermal cameras also find use in firefighting [63], face deidentification [64], human activity recognition (HAR) [65], occupancy estimation [66], disaster management [67], thermal overlay [25], and so on. Their use in artwork inspection to validate the authenticity and identify defects is also prominent [68]. Thermal fusion alongside RGB images has helped in the semantic segmentation of urban environments to assist autonomous vehicles [69]. Recent

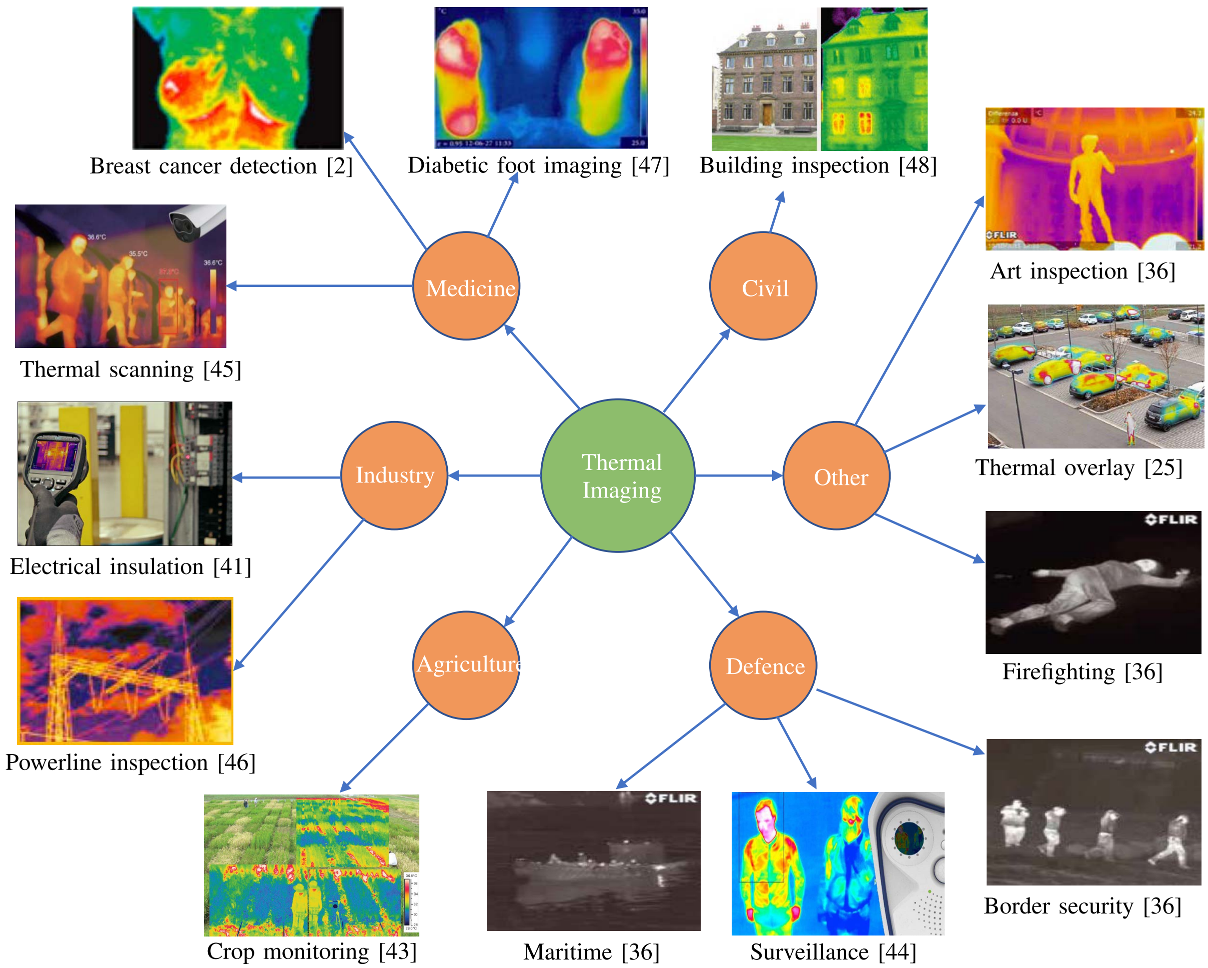

Fig. 3. Applications of thermal imaging.

advances in semiconductor technology coupled with enhanced computing capabilities and machine-learning algorithms have also helped to explore new applications for thermal cameras. Some of these will be covered in Section V.

V. Machine-Learning Techniques for Thermal Imaging Applications

In recent years, thermal imaging coupled with machine-learning techniques has gained traction. Thermal images provide the temperature gradient of the captured scene. Any fault or anomaly in a system or device is associated with a change in its temperature profile. By utilizing state-of-the-art machine-learning techniques along with thermal imaging, these anomalies can be easily detected and inferred in a contactless and noninvasive manner. Moreover, the ability to perform highly scalable operations on large datasets has also added to the popularity of using thermal imaging with machine-learning techniques.

In the electric power industry, identifying equipment faults early from the temperature distribution of thermal images can help prevent equipment failure, fire hazards, and other potential risks. Lin et al. [70] addresses the problem of incorrect detection of equipment parts with different orientations from hand-held thermal camera images. The authors propose a cascaded two-stage spatial transform network (STN) that is fed into faster region-based convolutional neural networks (R-CNNs) to identify the required rotation transformation. Training is performed separately for the two stages, and then further end-to-end fine-tuning is performed to achieve detection with large orientation angles. The proposed approach outperforms current state-of-the-art methods including the oriented you only look once (YOLO) algorithm with a higher mean average precision (mAP) value. Another work in [71] utilizes thermal imaging to characterize the condition of a machine. The authors use two CNNs along with the Zeiler method [72] to obtain useful insights from the thermal image. One of the CNNs is used to extract the spatial aspects from the roll-bearing element and the other CNN infers the gradation of imbalance using the extracted temporal features. The proposed system is able to obtain 91.6% and 95% accuracy for rotating machinery use cases in machine-fault detection and oil-level prediction applications. Another work by Choudhary et al. [73] focuses on detecting bearing faults in induction motors using thermal imaging. The performance of traditional feature extraction methods fails due to insignificant information and string noise from the thermal noise. The authors in this work thus use a 2-D discrete wavelet transform (2-D-DWT) along with principal component analysis (PCA) to resolve this issue. The extracted features were then arranged according to the Mahalanobis distance to select the optimal features. Classification is performed using support vector machines (SVMs), linear discriminant analysis (LDA), and complex decision trees (CDTs). Reported results show that SVM obtained higher classification accuracy when compared to other techniques. The work by Ogbechie et al. [74] uses dynamic Bayesian networks for anomaly detection in the laser surface heat treatment process. The proposed approach uses an NIT Tachyon 1024 thermal camera to obtain images of the heat treatment process. After the necessary preprocessing and feature selection, the data is trained using two different types of dynamic Bayesian networks with a k-fold cross-validation. An anomaly score is calculated that is used to identify and detect anomalies in the laser heat process.

Other fault detection and classification areas where thermal images combined with machine learning prove useful are in photovoltaic systems [75]. Photovoltaic systems are vulnerable to various defects such as encapsulant defects, back sheet defects, cracket cells, and faulty interconnections. In this work, the authors have initially performed a texture feature analysis for the different faulty panels using gray-level co-occurrence matrices (GLCMs). The extracted features are then trained using artificial neural networks (ANNs) to classify the faults. The new approach exhibits 93.4% training and 91.7% testing efficiency, respectively. It is also reported that the proposed approach outperforms other conventional techniques such as SVMs and k-nearest neighbors (kNNs) by a significant margin.

Machine learning is being extensively used in the medical domain to minimize manual decision making which can lead to errors. Machine-learning models once trained with the thermal images can be used to predict and detect tumors. Early cancer identification using noninvasive techniques with thermal imagery helps reduce the fatality rate. Karthiga and Narasimhan [82] studied various machine-learning classification techniques to best extract the features to display these cancer symptoms. Thermal imagery is initially preprocessed using top-hat and bottom-hat transforms. The resulting image structure is segmented using morphological operations to yield various statistical, geometrical, and intensity features. Further processing using GLCM is performed to obtain texture features. The texture features in the spatial domain are classified using various machine-learning techniques. The cubic SVM shows the most promising accuracy with 93.3% when compared to other techniques such as kNN, decision tree classifier, and logistic regression. Procházka et al. [79] use thermal cameras and heart rate sensors to study the time delay associated with various physiological functions of the body. The thermal camera provides facial images which are processed using a two-layer ANN to predict the actual change in breathing temperature. Additional adaptive algorithms are also with the heart rate measurements to accurately estimate the temperature. Results show that the time delay associated with the drop in heart rate and breathing frequency corroborates with real-world measurements obtained from the heart rate sensors of cyclists.

Other applications of thermal imagery coupled with machine learning include the detection of damaged pavements as studied in [80]. In this work, the authors use a pretrained EfficientNet B4 fusion architecture to combine thermal and RGB images to detect pavement damage. An argument dataset is also generated by the addition of camera noise, nonuniform illumination, and other parameters to replicate real-world pavement damages and scenarios. Experiments carried out with images from individual RGB sensors, thermal cameras, and fused images show that the fused thermal-RGB image provides better prediction accuracy of about 98.34%. The fused images are capable of providing reliable detections for various cracks such as alligator, longitudinal, and transverse along with pothole categories.

Li et al. [81] developed a novel approach to enable semantic segmentation for thermal images by introducing a gated featurewise transform layer to the proposed edge-conditioned CNN (EC-CNN) architecture. Low-resolution thermal images are affected by thermal crossover and imaging noise that makes detecting object boundaries challenging. To overcome this issue, the authors utilize hierarchical edge features obtained by training RGB images. The trained model is then fed to the proposed semantic segmentation network that is based on DeepLabv3 [88]. The reported results show that the proposed method outperforms traditional methods for thermal image semantic segmentation. Additionally, the authors have also provided a manually annotated thermal image dataset (SODA) for further research into thermal semantic segmentation. Another interesting work by Huo et al. [87] utilizes the transmission properties of IR to segment images containing glass elements. As glass is transparent to visible light, traditional methods for RGB images fail to effectively detect and segment regions containing glass. The architecture in the proposed work is made up of two independent ResNet-50 networks that act as the encoder stage for extracting high-level features from both the RGB and thermal images. These features are then combined using a transformer-based fusion module. The result is then fed into a decoder for obtaining the desired segmentation output. Qualitative and quantitative evaluations have shown that the proposed approach outperforms current state-of-the-art techniques and effectively segments glass components in images. However, the approach still requires further work to classify in polarized image conditions.

Occupancy estimation is another potential application based on thermal imagery. Chidurala and Li [66] provided a comparative study of various low-resolution thermal sensors, GridEye, MLX90640, and Lepton that can be used to provide highly accurate real-time occupancy estimation. The proposed approach involves a unified algorithm pipeline that involves noise reduction, bilinear interpolation, blob filtering to distinguish multiple people close to each other, and connected component analysis to obtain the best possible results. The output from this pipeline is fed into a novel feature vector design that is used in conjunction with classification algorithms to classify target occupants. Classification algorithms include random forests, Gaussian naive Bayes, kNNs, and SVM. Experimental results have reported that the random forests algorithm exhibits 99% accuracy. In comparison to the above, Tyndall et al. [77] used a low-pixel count 4×16 thermal detector array to perform occupancy detection. The thermal detector along

TABLE VI
MACHINE-LEARNING TECHNIQUES FOR THERMAL IMAGING

Year	Method	Application	References	Comments
2016	Bayesian networks	Firefighting	[76]	1) Combination of mean, dissimilarity, correlation, skewness, and standard deviation produced highest performance results. 2) Usage of CNN and discrete wavelet transforms can be explored.
2016	K* algorithm	Occupancy estimation	[77]	1) Entropy-based algorithms exhibited excellent performance. 2) Can improve classification performance using recent occupancy history.
2017	Dynamic bayesian networks	Anomaly detection	[74]	1) Obtained 90% specificity with greater than 80% sensitivity. 2) Can improve process parameter values. Online implementation for timely feedback can also be a potential future work.
2017	Dynamic bayesian networks	Occupancy estimation	[78]	1) Three order reduction in memory requirement and 8x reduction in memory utilization. 13x improvement in execution time. 2) Future extension can include exploring the performance with multiple PIR sensors.
2018	STN, Faster R-CNN	Equipment detection	[70]	1) Accurate identification of rotated equipments. 2) Future extension can be online implementation for live detection.
2018	CNN	Condition monitoring of machines	[71]	1) More than 90% accuracy in real-world applications. 2) Online condition monitoring for offshore wind turbines can be future work.
2018	ANNs	Breathing frequency estimation	[79]	1) Results corroborate with real values obtained from cycling expeditions. 2) Usage of CNNs and parallel algorithms for future work.
2019	ANNs	Identifying faults in photovoltaic systems	[75]	1) Fast detection time along with remote monitoring. Enhanced classification accuracy of 92.8% with ANNs as compared to SVMs and kNNs. 2) Online methods and CNNs can be explored.
2019	Deep RNN based LSTM	Human activity recognition	[65]	1) HAR systems with RNNs offer 96% accuracy as compared to other methods. 2) Performance with bright images, oriented/tilted subjects, etc can also be explored.
2020	EfficientNet B4	Pavement defect detection	[80]	1) Excellent pavement defect detection performance compared to other methods. Additionally, the proposed method outperforms detection as compared to RGB images. 2) Prediction performance is low for road marking, manholes, and shadow as compared to RGB.
2020	Gated featurewise transform with EC-CNN	Thermal semantic segmentation	[81]	1) Proposed method performs better than DeepLabv3 with 4.8% gain. Resonable performance under thermal crossover. 2) Incorporate transfer learning from RGB data and including more annotated thermal images can be future work.
2020	Random forests and ensemble learning	Face recognition and de-identification	[64]	1) Ensemble learning can improve the prediction performance. 2) Fusion techniques can be investigated.
2021	SVM, LDA, CDT	Induction motor fault detection	[73]	1) SVM outperformed LDA and CDT for bearing defect classification. 2) Can increase cases for bearing defects.
2021	Cubic SVM	Breast cancer identification	[82]	1) Cubic SVM classifier produced highest accuracy of 93.9% as compared to other classifiers. 2) The work can be extended to include other views such as right, left, and lateral to improve accuracy.
2021	CNN	Hand gesture classification	[83]	1) Lightweight CNNs with high accuracy of 99.52% 2) Can extend for hand gesture recognition in complex backgrounds.
2021	ResNet-50 with random forest	Pollution identification on MOSA	[84]	1) Proposed approach uses ResNet50 with random forest to achieve mean recognition accuracy of 98.04%. 2) Experiments on real MOSA samples can be performed.
2021	Random forest	Occupancy estimation	[66]	1) Uses blob filtering algorithm to distinguish humans close to each other. Achieves 99% accuracy. 2) Sensor fusion, different deployment configurations, transient heat conditions, CNNs and RNNs can be explored.
2021	Deep convolutional encoder-decoder network with adaptive boost	Occupancy estimation	[85]	1) Privacy-friendly, low-resolution TSA sensing technique with 98.43% classification accuracy. 2) Estimating human-sensor distance using entropy point methods can be potential future work.
2021	ResNet encoder-decoder network with pyramid supervision training	Semantic segmentation in snowy environment	[86]	1) Proposed network achieved 78% mIoU and has become state-of-the-art for snowy environments. 2) Dataset classes can include additional classes such as animals and maintenance holes. Integrate other sensors for future work.
2022	ResNet-50 encoder decoder model with transformer based fusion	Glass segmentation	[87]	1) Proposed RGB-T network outperformed existing methods with 93.8% IoU for images with glass. 2) Can combine with polarization to improve result.

with the RGB camera is mounted on the Raspberry Pi to obtain the images. The RGB camera served as the ground-truth occupancy values. The background separation algorithm coupled with a slow-moving exponential weighted moving average (EMWA) accompanied the preprocessing stage before feature extraction. Three features—number of active pixels, number of connected components, and size of the largest connected component—were identified to be used with the classification algorithms. The Weka toolchain [89] was used to compare different machine-learning classification algorithms. It was found that entropy-based algorithms such as K* gave the best performance with an accuracy of 82.56% and a root mean square error of 0.304. Another approach followed by Naser et al. [85] uses an array of thermal sensors at different locations of the room to perform human segmentation and occupancy estimation. In this work, the authors have proposed a deep convolutional encoder–decoder network for human segmentation from thermal images. Residual thermal signatures are further eliminated during the postprocessing using connectivity filters. To classify and also to determine occupancy estimation, the output is then fed to an adaptive boosting algorithm. The adaptive boosting approach provides an accuracy of 98.43% from vertical and 100% from overhead sensor locations. Another work by Leech et al. [78] uses a Bayesian machine-learning algorithm on a resource-constrained ARM Cortex-Mo-based ST Nucleo-F070RB board to estimate the room occupancy using a single analog passive infrared (PIR) sensor. The proposed algorithm uses an infinite hidden Markov model (iHMM) with Laplace components on the raw PIR data for segmentation. The segmented data is now manipulated to estimate the Laplace diversity which indicates the room occupancy. Reported results show that a moderately high-performance microcontroller is able to house the occupancy algorithm, while providing real-time performance and reduced power consumption.

Classification of hand gestures for sign language digits can also be performed using thermal imaging as demonstrated in [83]. Daniel et al. [83] demonstrated an end-to-end edge computing system based on lightweight CNNs that can classify thermal images of different hand gestures. The proposed approach utilizes a 3200 thermal image dataset to train a model that is based on bottleneck layers. The model is deployed on a Raspberry Pi and the developed system achieves 99.52% accuracy. Furthermore, the proposed approach is compared with the Big Transfer (BiT) model to report approximately a 20% improvement in accuracy. For HAR, Zia Uddin et al. [65] extend the OpenPose approach to extract body joints from human thermal images for activity recognition. The proposed approach utilizes OpenPose and subsequently performs a spatiotemporal feature extraction. Discriminant analysis is performed on the extracted features followed by a deep recurrent neural network (RNN)-based long short-term memory (LSTM) to better retain the embedded time-sequential information. The novel approach is reported to outperform other techniques such as HMMs, deep belief networks (DBNs), CNNs, and RNNs. Thermography is also used for face recognition and deidentification [64]. Normal RGB images can easily deceive face recognition systems as they work only on identifying the extracted features. The authors in this work use additional features extracted from thermal images such as feature matrix and feature image along with random forests and ensemble learning to improve prediction accuracy and better facial deidentification. This can help in preventing erroneous face recognition with the use of facial images. Another interesting work in [76] uses thermal imagery in firefighting situations to identify local conditions and decide the proper navigation course through a fire or smoke-prone area. High-temperature regions are separated using the Otsu method which is then fed into a Bayesian classifier to probabilistically detect multiple classes during real-time implementation. Furthermore, a multiobjective genetic algorithm using resubstitution and cross-validation errors is also used to find the best combination of features to obtain the lowest error and highest performance.

Improving road safety in snowy environments is yet another application in which thermal imagery can be beneficial. Vachmanus et al. [86] have developed a multimodal RGB-thermal fusion model for the semantic segmentation of roads in snow-filled environments. The architecture utilizes a convolutional encoder–decoder fusion network where the encoder is based on a fully preactivated ResNet-50 model [90] to maintain a good tradeoff between computation and feature learning. Both the RGB and thermal images are fed into the encoder module that is followed by an atrous spatial pyramid pooling (ASPP) which is used to incorporate image features. The ASPP's output is fused and then fed into a ResNet-34-based decoder module. An additional pyramid supervision training scheme [91] is also employed to improve training accuracy. The proposed method has obtained a 78% mean intersection over union (mIoU) outperforming state-of-the-art network for snowy environments. Thermal imaging coupled with machine learning is also used to identify the severity of pollution on metal oxide surge arrester (MOSA) [84]. The proposed approach utilizes thermal images of MOSA at various pollution levels, which are fed into pretrained "ResNet50" architecture for feature extraction. The extracted features are then given to various classifiers such as kNN, SVM, naive Bayes, and random forest. Random forest gave the best accuracy along with fast inference time. The authors were also able to validate the practicality of the proposed approach by experimenting on 11-kV MOSA which also gave accurate results. A brief summary of the various machine-learning techniques used for thermal imaging can be found in Table VI.

VI. Conclusion and Future Work

Technological innovations in the semiconductor industry and along with other advancements have made thermal imaging applications more accessible and prevalent. Novel machine-learning algorithms in thermal imaging applications have been shown to provide better performance when compared to their traditional counterparts. Thermal fusion has shown to be used in various application scenarios and is still an active research topic. Combining polarization properties in thermal fusion algorithms containing glass segments is still unexplored. Furthermore, it is shown above that offline algorithms for thermal data provide good performance. However, their online implementations require further research. In object detection and classification, eliminating the thermal retention signatures is also crucial to improve performance. Furthermore, the current algorithms utilize existing implementations for normal RGB with some variations. To obtain better performance and efficient resource utilization, devising or modifying the algorithms to incorporate the thermal characteristics of the scene would be highly beneficial.

In this article, the most recent developments in thermal imaging are reviewed. The key specifications of the most recent thermal imaging devices have been discussed. The use of thermal imaging in a wide range of disciplines and scenarios was discussed. Finally, machine-learning techniques for thermal imaging were discussed along with possible future work. This article is useful as a reference guide for designing and implementing thermal imaging-based systems and/or applications.

References

[1] A. Berg, "Detection and tracking in thermal infrared imagery," Ph.D. dissertation, Dept. Elect. Eng., Linköping Univ. Electron. Press, Linköping Univ., Linköping, Sweden, 2016.
[2] P. Rajmanova, P. Nudzikova, and D. Vala, "Application and technology of thermal imagine camera in medicine," *IFAC-PapersOnLine*, vol. 48, no. 4, pp. 492–497, 2015.
[3] R. C. Gonzalez et al., *Digital Image Processing*, vol. 455, 2nd ed. Beijing, China: Publishing House of Electronics Industry, 2002.
[4] *Megger—Introduction to Thermal Imaging*. Accessed: Nov. 2022. [Online]. Available: https://d20g1hcwzqzdjk.cloudfront.net/sites/www.voltimum.pt/files/fields/attachment_file/introduction-thermography-en_v01.pdf
[5] N. I. Hristov, M. Betke, and T. H. Kunz, "Applications of thermal infrared imaging for research in aeroecology," *Integrative Comparative Biol.*, vol. 48, no. 1, pp. 50–59, Jul. 2008.
[6] S. Lin, "Monitoring of thermal processes for medical applications using infrared thermography," Ph.D. dissertation, Dept. Elect. Eng. Comput. Sci., Graduate School Vanderbilt Univ., Nashville, TN, USA, 2017.
[7] J. Marins et al., "Applications of infrared thermography in sports. A review," *Int. J. Med. Sci. Phys. Activity Sport*, vol. 15, no. 60, pp. 805–824, 2013.
[8] B. Wiecek, "Review on thermal image processing for passive and active thermography," in *Proc. IEEE Eng. Med. Biol.*, Shanghai, China, Jan. 2005, pp. 686–689.
[9] B. Kateb, V. Yamamoto, C. Yu, W. Grundfest, and J. P. Gruen, "Infrared thermal imaging: A review of the literature and case report," *NeuroImage*, vol. 47, pp. T154–T162, Aug. 2009.
[10] R. Ishimwe et al., "Applications of thermal imaging in agriculture—A review," *Adv. Remote Sens.*, vol. 3, no. 3, p. 128, Sep. 2014.
[11] W. Yongqing, G. Zongqing, W. Shuonan, and H. Ping, "The temperature measurement technology of infrared thermal imaging and its applications review," in *Proc. 13th IEEE Int. Conf. Electron. Meas. Instrum. (ICEMI)*, Yangzhou, China, Oct. 2017, pp. 401–406.
[12] O. M. Rajpurkar, S. S. Kamble, J. P. Nandagiri, and P. J. Bide, "A survey on engagement and emotion analysis in theatre using thermal imaging," in *Proc. 4th Int. Conf. Electron., Commun. Aerosp. Technol. (ICECA)*, Coimbatore, India, Nov. 2020, pp. 905–911.
[13] A. Hakim and R. N. Awale, "Thermal imaging–An emerging modality for breast cancer detection: A comprehensive review," *J. Med. Syst.*, vol. 44, no. 8, pp. 1–18, Jul. 2020.
[14] T. X. B. Nguyen, K. Rosser, and J. Chahl, "A review of modern thermal imaging sensor technology and applications for autonomous aerial navigation," *J. Imag.*, vol. 7, no. 10, p. 217, Oct. 2021.
[15] A. A. Gowen, B. K. Tiwari, P. J. Cullen, K. McDonnell, and C. P. O'Donnell, "Applications of thermal imaging in food quality and safety assessment," *Trends Food Sci. Technol.*, vol. 21, no. 4, pp. 190–200, 2010.
[16] *KEMET QMS Pyroelectric IR Motion Sensor*. Accessed: Nov. 2022. [Online]. Available: https://content.kemet.com/datasheets/KEM_SE0212_QMS.pdf
[17] A. W. Van Herwaarden and P. M. Sarro, "Thermal sensors based on the Seebeck effect," *Sens. Actuators A, Phys.*, vol. 10, nos. 3–4, pp. 321–346, Nov. 1986.
[18] *Omron D6T MEMS Thermal Sensor—Datasheet*. Accessed: Nov. 2022. [Online]. Available: https://components.omron.com/us-en/ds_related_pdf/A284-E1.pdf
[19] *FLIR Lepton 3.5 Thermal Camera*. Accessed: Nov. 2022. [Online]. Available: https://www.flir.eu/products/lepton/?model=500-0771-01
[20] *PYROSENS—Datasheet*. Accessed: Nov. 2022. [Online]. Available: http://www.dias-infrared.de/pdf/pyrosens_arrays_eng_mail.pdf
[21] *Seek Thermal InspectionCAM—Datasheet*. Accessed: Nov. 2022. [Online]. Available: https://www.thermal.com/uploads/1/0/1/3/101388544/inspectioncam_-_spec_sheet_v3.pdf
[22] *Evo Thermal 90—Datasheet*. Accessed: Nov. 2022. [Online]. Available: https://terabee.b-cdn.net/wp-content/uploads/2020/10/TeraRanger-Evo-Thermal-Specsheet-1.pdf
[23] C. Gobbi, "Low cost thermal imaging system for welding applications," M.S. thesis, Dept. Mech. Mechtron. Eng., Univ. Waterloo, Waterloo, ON, Canada, 2016.
[24] G. Guglielmo and M. Klincewicz, "The temperature of morality: A behavioral study concerning the effect of moral decisions on facial thermal variations in video games," in *Proc. 16th Int. Conf. Found. Digit. Games (FDG)*, New York, NY, USA, Aug. 2021, pp. 1–4.
[25] *MOBOTIX Thermal Solutions*. Accessed: Nov. 2022. [Online]. Available: https://d347awuzx0kdse.cloudfront.net/vsp/content-file/mx_thermal_technology_en_200406_web.pdf
[26] *Compact Thermal Camera FLIR C5*. Accessed: Nov. 2022. [Online]. Available: https://www.flir.eu/products/c5/?vertical=condition%20monitoring&segment=solutions
[27] *FLUKE—Fluke Ti480 PRO Infrared Camera*. Accessed: Nov. 2022. [Online]. Available: https://www.fluke.com/en/product/thermal-cameras/ti480-pro
[28] *SEEK Thermal—CompactPRO XR*. Accessed: Nov. 2022. [Online]. Available: https://www.thermal.com/compact-series.html
[29] *PULSAR—HELION 2 XP PRO Thermal Imaging Monoculars*. Accessed: Jun. 2022. https://www.pulsar-nv.com/glo/products/33/thermal-imaging-scopes/helion-version-2/
[30] *CAT—Cat S62 Pro*. Accessed: Nov. 2022. [Online]. Available: https://www.catphones.com/en-gb/cat-s62-pro-smartphone/
[31] *PULSAR—MERGER LRF Thermal Imaging Binoculars*. Accessed: Nov. 2022. [Online]. Available: https://www.pulsar-nv.com/glo/products/33/thermal-imaging-binoculars/merger/
[32] *FLUKE—Fluke RSE600 Mounted Infrared Camera*. Accessed: Nov. 2022. [Online]. Available: https://www.fluke.com/en/product/thermal-cameras/rse600
[33] *MOBOTIX M16 Thermal TR—Datasheet*. Accessed: Nov. 2022. [Online]. Available: https://www.mobotix.com/sites/default/files/2022-08/Mx_TS_M16B_V1.05_EN_20220811.pdf
[34] *MOBOTIX S16 DualFlex—Datasheet*. Accessed: Nov. 2022. [Online]. Available: https://www.mobotix.com/sites/default/files/2022-08/Mx_TS_S16B_V1.05_EN_20220811.pdf
[35] *FLIR Thermal Imaging Cameras for Predictive Maintenance*. Accessed: Nov. 2022. [Online]. Available: https://assets.tequipment.net/assets/1/7/FLIR-Predictive-Maintenance-Brochure-7038_EN.pdf
[36] *FLIR Imaging for Building Diagnostics*. Accessed: Nov. 2022. [Online]. Available: https://www.flirmedia.com/MMC/THG/Brochures/T820484/T820484_EN.pdf
[37] *MOBOTIX—MOBOTIX M16 Thermal*. Accessed: Nov. 2022. [Online]. Available: https://www.mobotix.com/en/products/thermographic-cameras/m16-thermal
[38] *MOBOTIX—MOBOTIX M16 Thermal TR*. Accessed: Nov. 2022. [Online]. Available: https://www.mobotix.com/en/products/thermographic-cameras/m16-thermal-tr
[39] *MOBOTIX—MOBOTIX S16 Dual Flex*. Accessed: Nov. 2022. [Online]. Available: https://www.mobotix.com/index.php/en/products/outdoor-cameras/s16-dualflex
[40] *MOBOTIX—MOBOTIX S16 Thermal TR*. Accessed: Nov. 2022. [Online]. Available: https://www.mobotix.com/index.php/en/products/thermographic-cameras/s16-thermal-tr
[41] *FLIR 12 Things to Know*. Accessed: Nov. 2022. [Online]. Available: https://www.flir.com/landing/instruments/12-things-to-know-before-buying-a-thermal-camera/
[42] *Thermal Imaging for Science/R&D*. Accessed: Nov. 2022. [Online]. Available: https://www.flirmedia.com/MMC/THG/Brochures/T820486/T820486_EN.pdf
[43] H. G. Jones et al., "Thermal infrared imaging of crop canopies for the remote diagnosis and quantification of plant responses to water stress in the field," *Funct. Plant Biol.*, vol. 36, no. 11, pp. 978–989, Nov. 2009.
[44] *Surveillance Secure*. Accessed: Nov. 2022. [Online]. Available: https://surveillancesecure.com/thermal-surveillance-cameras-provide-proactive-warning-with-temperature-imaging-technology/

[45] *Platinum CCTV—Skin Temperature Measurement*. Accessed: Nov. 2022. [Online]. Available: https://platinumcctv.com/bf3221-skin-temp-thermal-camera

[46] *FLIR Thermal Imaging Guidebook for Industrial Applications*. Accessed: Nov. 2022. [Online]. Available: https://www.flirmedia.com/MMC/THG/Brochures/T820264/T820264_EN.pdf

[47] S. Shaikh, N. Akhter, and R. Manza, "Current trends in the application of thermal imaging in medical condition analysis," *Int. J. Innov. Technol. Explor. Eng*, vol. 8, no. 8, pp. 2708–2712, Jun. 2019.

[48] I. Thusyanthan, T. Blower, and W. Cleverly, "Innovative uses of thermal imaging in civil engineering," in *Proc. Inst. Civil Eng.*, vol. 170, no. 2, Apr. 2017, pp. 81–87.

[49] B. Miethig, A. Liu, S. Habibi, and M. V. Mohrenschildt, "Leveraging thermal imaging for autonomous driving," in *Proc. IEEE Transp. Electrific. Conf. Expo (ITEC)*, Detroit, MI, USA, Jun. 2019, pp. 1–5.

[50] D. Savasci and M. Ceylan, "Thermal image analysis for neonatal intensive care units (first evaluation results)," in *Proc. 26th Signal Process. Commun. Appl. Conf. (SIU)*, Izmir, Turkey, May 2018, pp. 1–4.

[51] S. Mambou, P. Maresova, O. Krejcar, A. Selamat, and K. Kuca, "Breast cancer detection using infrared thermal imaging and a deep learning model," *Sensors*, vol. 18, no. 9, p. 2799, Aug. 2018.

[52] V. Tanriverdi and N. G. Gencer, "Induced current thermal imaging in breast cancer detection," in *Proc. 29th Signal Process. Commun. Appl. Conf. (SIU)*, Istanbul, Turkey, Jun. 2021, pp. 1–4.

[53] S. Shaikh et al., "Segmentation of thermal images using thresholding-based methods for detection of malignant tumours," in *Proc. Intell. Syst. Technol. Appl.*, Jaipur, India, 2016, pp. 131–146.

[54] S. Quinn et al., "A thermal imaging solution for early detection of pre-ulcerative diabetic hotspots," in *Proc. Annu. Int. Conf. IEEE Eng. Med. Biol. Soc. (EMBC)*, Berlin, Germany, 2019, pp. 1737–1740.

[55] R. Y. Brzezinski et al., "Automated processing of thermal imaging to detect COVID-19," *Sci. Rep.*, vol. 11, no. 1, pp. 1–10, Sep. 2021.

[56] D. Selvathi and K. Suganya, "Support vector machine based method for automatic detection of diabetic eye disease using thermal images," in *Proc. 1st Int. Conf. Innov. Inf. Commun. Technol. (ICIICT)*, Chennai, India, Apr. 2019, pp. 1–6.

[57] S. E. Godoy et al., "Detection theory for accurate and non-invasive skin cancer diagnosis using dynamic thermal imaging," *Biomed. Opt. Exp.*, vol. 8, no. 4, pp. 2301–2323, Apr. 2017.

[58] V. Yang et al., "Thermal imaging of root caries in vivo," *J. dental Res.*, vol. 99, no. 13, pp. 1502–1508, Aug. 2020.

[59] F. Svanstrom, C. Englund, and F. Alonso-Fernandez, "Real-time drone detection and tracking with visible, thermal and acoustic sensors," in *Proc. 25th Int. Conf. Pattern Recognit. (ICPR)*, Milan, Italy, Jan. 2021, pp. 7265–7272.

[60] T. Sosnowski et al., "Thermovision system for aircraft landing," *Meas. Autom. Monitor.*, vol. 61, pp. 180–183, Jul. 2015.

[61] D. ALshukri, V. L. R, S. E. P, and P. Krishnan, "Intelligent border security intrusion detection using IoT and embedded systems," in *Proc. 4th MEC Int. Conf. Big Data Smart City (ICBDSC)*, Muscat, Oman, Jan. 2019, pp. 1–3.

[62] A. Fernandez, A. Souto, C. Gonzalez, and R. Mendez-Rial, "Embedded vision system for monitoring arc welding with thermal imaging and deep learning," in *Proc. Int. Conf. Omni-layer Intell. Syst. (COINS)*, Barcelona, Spain, Aug. 2020, pp. 1–6.

[63] M. Bhattarai and M. Martinez-Ramon, "A deep learning framework for detection of targets in thermal images to improve firefighting," *IEEE Access*, vol. 8, pp. 88308–88321, 2020.

[64] C.-H. Lin, Z.-H. Wang, and G.-J. Jong, "A de-identification face recognition using extracted thermal features based on deep learning," *IEEE Sensors J.*, vol. 20, no. 16, pp. 9510–9517, Apr. 2020.

[65] M. Z. Uddin, W. Khaksar, and J. Torresen, "A thermal camera-based activity recognition using discriminant skeleton features and RNN," in *Proc. Int. Conf. Ind. Inform. (INDIN)*, Helsinki, Finland, vol. 1, 2019, pp. 777–782.

[66] V. Chidurala and X. Li, "Occupancy estimation using thermal imaging sensors and machine learning algorithms," *IEEE Sensors J.*, vol. 21, no. 6, pp. 8627–8638, Mar. 2021.

[67] A. Arunraj et al., "An IoT application in disaster management using real-time thermal imaging system," in *Proc. AIP Conf.*, Kollam, India, vol. 2222, no. 1, Apr. 2020, Art. no. 030025.

[68] M. Rippa et al., "Active thermography for non-invasive inspection of an artwork on poplar panel: Novel approach using principal component thermography and absolute thermal contrast," *J. Nondestruct. Eval.*, vol. 40, no. 1, pp. 1–9, Feb. 2021.

[69] Y. Sun, W. Zuo, and M. Liu, "RTFNet: RGB-thermal fusion network for semantic segmentation of urban scenes," *IEEE Robot. Autom. Lett.*, vol. 4, no. 3, pp. 2576–2583, Mar. 2019.

[70] Y. Lin, M. Wang, C. Gu, J. Qin, D. Bai, and J. Li, "A cascaded spatial transformer network for oriented equipment detection in thermal images," in *Proc. 2nd IEEE Conf. Energy Internet Energy Syst. Integr. (EI)*, Beijing, China, Oct. 2018, pp. 1–5.

[71] O. Janssens, R. Van de Walle, M. Loccufier, and S. Van Hoecke, "Deep learning for infrared thermal image based machine health monitoring," *IEEE/ASME Trans. Mechatronics*, vol. 23, no. 1, pp. 151–159, Feb. 2018.

[72] M. D. Zeiler and R. Fergus, "Visualizing and understanding convolutional networks," in *Proc. ECCV*, Zurich, Switzerland, 2014, pp. 818–833.

[73] A. Choudhary, D. Goyal, and S. S. Letha, "Infrared thermography-based fault diagnosis of induction motor bearings using machine learning," *IEEE Sensors J.*, vol. 21, no. 2, pp. 1727–1734, Aug. 2021.

[74] A. Ogbechie, J. Díaz-Rozo, P. Larrañaga, and C. Bielza, "Dynamic Bayesian network-based anomaly detection for in-process visual inspection of laser surface heat treatment," in *Machine Learning for Cyber Physical Systems*, J. Beyerer, O. Niggemann, and C. Kühnert, Eds. Berlin, Germany: Springer, 2017, pp. 17–24.

[75] V. S. B. Kurukuru, A. Haque, M. A. Khan, and A. K. Tripathy, "Fault classification for photovoltaic modules using thermography and machine learning techniques," in *Proc. Int. Conf. Comput. Inf. Sci. (ICCIS)*, Sakaka, Saudi Arabia, Apr. 2019, pp. 1–6.

[76] J.-H. Kim, S. Jo, and B. Y. Lattimer, "Feature selection for intelligent firefighting robot classification of fire, smoke, and thermal reflections using thermal infrared images," *J. Sensors*, vol. 2016, pp. 1–13, Sep. 2016.

[77] A. Tyndall, R. Cardell-Oliver, and A. Keating, "Occupancy estimation using a low-pixel count thermal imager," *IEEE Sensors J.*, vol. 16, no. 10, pp. 3784–3791, Feb. 2016.

[78] C. Leech, Y. P. Raykov, E. Ozer, and G. V. Merrett, "Real-time room occupancy estimation with Bayesian machine learning using a single PIR sensor and microcontroller," in *Proc. IEEE Sensors Appl. Symp. (SAS)*, Mar. 2017, pp. 1–6.

[79] A. Procházka, H. Charvátová, S. Vaseghi, and O. Vyšata, "Machine learning in rehabilitation assessment for thermal and heart rate data processing," *IEEE Trans. Neural Syst. Rehabil. Eng.*, vol. 26, no. 6, pp. 1209–1214, Apr. 2018.

[80] C. Chen, S. Chandra, Y. Han, and H. Seo, "Deep learning-based thermal image analysis for pavement defect detection and classification considering complex pavement conditions," *Remote Sens.*, vol. 14, no. 1, p. 106, Dec. 2021.

[81] C. Li, W. Xia, Y. Yan, B. Luo, and J. Tang, "Segmenting objects in day and night: Edge-conditioned CNN for thermal image semantic segmentation," *IEEE Trans. Neural Netw. Learn. Syst.*, vol. 32, no. 7, pp. 3069–3082, Jul. 2021.

[82] R. Karthiga and K. Narasimhan, "Medical imaging technique using curvelet transform and machine learning for the automated diagnosis of breast cancer from thermal image," *Pattern Anal. Appl.*, vol. 24, no. 3, pp. 981–991, Feb. 2021.

[83] D. S. Breland, S. B. Skriubakken, A. Dayal, A. Jha, P. K. Yalavarthy, and L. R. Cenkeramaddi, "Deep learning-based sign language digits recognition from thermal images with edge computing system," *IEEE Sensors J.*, vol. 21, no. 9, pp. 10445–10453, Feb. 2021.

[84] A. K. Das, D. Dey, B. Chatterjee, and S. Dalai, "A transfer learning approach to sense the degree of surface pollution for metal oxide surge arrester employing infrared thermal imaging," *IEEE Sensors J.*, vol. 21, no. 15, pp. 16961–16968, Aug. 2021.

[85] A. Naser, A. Lotfi, and J. Zhong, "Adaptive thermal sensor array placement for human segmentation and occupancy estimation," *IEEE Sensors J.*, vol. 21, no. 2, pp. 1993–2002, Jan. 2021.

[86] S. Vachmanus, A. A. Ravankar, T. Emaru, and Y. Kobayashi, "Multi-modal sensor fusion-based semantic segmentation for snow driving scenarios," *IEEE Sensors J.*, vol. 21, no. 15, pp. 16839–16851, Aug. 2021.

[87] D. Huo, J. Wang, Y. Qian, and Y.-H. Yang, "Glass segmentation with RGB-thermal image pairs," 2022, *arXiv:2204.05453*.

[88] *DeeplabV3*. Accessed: Nov. 2022. [Online]. Available: https://pytorch.org/hub/pytorch_vision_deeplabv3_resnet101/

[89] *Weka*. Accessed: Nov. 2022. [Online]. Available: http://www.cs.waikato.ac.nz/ml/weka/

[90] K. He, X. Zhang, S. Ren, and J. Sun, "Deep residual learning for image recognition," in *Proc. IEEE Conf. Comput. Vis. Pattern Recognit. (CVPR)*, Las Vegas, NV, USA, Jun. 2016, pp. 770–778.

[91] J. Jiang, L. Zheng, F. Luo, and Z. Zhang, "RedNet: Residual encoder–decoder network for indoor RGB-D semantic segmentation," 2018, *arXiv:1806.01054*.

A. N. Wilson received the B.Tech. degree in electronics and communication engineering from the Government Model Engineering College, Kochi, India, in 2012, and the M.Tech. degree from the Indian Institute of Technology Bombay, Mumbai, India, in 2016. He is currently pursuing the Ph.D. degree with the Department of ICT, University of Agder, Grimstad, Norway.

His research interests include the different aspects of radar signal processing, machine learning for autonomous cyber-physical systems, and wireless communications.

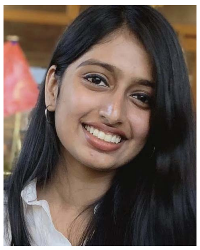

Khushi Anil Gupta received the bachelor's degree in electrical and electronics (EEE) from the Birla Institute of Technology and Science (BITS) Pilani, Hyderabad, India, in 2022. She is currently pursuing the master's degree in computer engineering with Columbia University, New York, NY, USA.

She was a Visiting Student Researcher with the ACPS Research Group, University of Agder (UiA), Grimstad, Norway. Her research interests include deep learning, computer networks, the Internet of Things (IoT), computer architecture, computer vision, and embedded systems.

Balu Harshavardan Koduru received the bachelor's degree in electronics and instrumentation and the master's degree in physics (integrated dual degree) from the Birla Institute of Technology and Science Pilani (BITS Pilani), Pilani, India, in 2022. He is currently pursuing the master's degree in artificial intelligence with the State University of New York at Buffalo, Buffalo, NY, USA.

He was a Visiting Master's Student with the University of Agder, Grimstad, Norway, while pursuing the integrated dual degree. His research interests include the application of machine learning, deep learning, reinforcement learning, computer vision for robotics, and autonomous cyber-physical systems.

Abhinav Kumar (Senior Member, IEEE) received the B.Tech., M.Tech., and Ph.D. degrees in electrical engineering from the Indian Institute of Technology Delhi, New Delhi, India, in 2009 and 2013, respectively.

From September to November 2013, he was a Research Associate with the Indian Institute of Technology Delhi. From December 2013 to November 2014, he was a Postdoctoral Fellow with the University of Waterloo, Waterloo, ON, Canada. Since November 2014, he has been with the Indian Institute of Technology Hyderabad, Hyderabad, India, where he is currently an Associate Professor. His research interests include the different aspects of wireless communications and networking.

Ajit Jha was born in Nepal in 1984. He received the B.Sc. degree in electronics and communication engineering from Khulna University, Khulna, Bangladesh, in 2007, the European master's degree in photonic networks from Aston University, Birmingham, U.K., and Scuola Superiore Sant Anna, Pisa, Italy, in 2012, and the Ph.D. degree from the Technical University of Catalunya, Barcelona, Spain, and the Karlsruhe Institute of Technology, Karlsruhe, Germany, in 2016.

From 2016 to 2019, he worked with various industries related to autonomous vehicles working on innovative technologies, such as Automotive ethernet, ADAS, surround view systems, camera mirror systems, and blind sport warning, to name a few. He is currently an Associate Professor of Mechatronics with the Department of Engineering Sciences, University of Agder, Grimstad, Norway. He has (co)authored more than 20 articles and holds two patents. His research interests include sensors, sensor fusion, image/signal processing, ML, ADAS functionalities toward autonomous systems, and the Internet of Things.

Dr. Jha is a recipient of the Erasmus Mundus Masters Course (EMMC) and Erasmus Mundus Joint Doctorate (EMJD) both funded by the European Union (EU). In addition, he has been an active reviewer and a member of the technical program committee of numerous international peer-reviewed journals and conferences.

Linga Reddy Cenkeramaddi (Senior Member, IEEE) received the master's degree in electrical engineering from the Indian Institute of Technology Delhi (IIT Delhi), New Delhi, India, in 2004, and the Ph.D. degree in electrical engineering from the Norwegian University of Science and Technology (NTNU), Trondheim, Norway, in 2011.

He was with Texas Instruments, Dallas, TX, USA, where he was involved in mixed-signal circuit design before joining the Ph.D. Program at NTNU. After finishing the Ph.D. degree, he worked on radiation imaging for an atmosphere–space interaction monitor (ASIM mission to the International Space Station) at the University of Bergen, Bergen, Norway, from 2010 to 2012. He is currently the Leader of the Autonomous and Cyber-Physical Systems (ACPS) Research Group and a Professor with the University of Agder, Grimstad, Norway. He has coauthored over 120 research publications that have been published in prestigious international journals and standard conferences. His main scientific interests include cyber-physical systems, autonomous systems, and wireless embedded systems.

Dr. Cenkeramaddi is also a member of the editorial boards of various international journals and the technical program committees of several IEEE conferences. Several of his master students received the best master thesis awards in information and communication technology (ICT). He is the Principal Investigator and a Co-Principal Investigator of many research grants from the Norwegian Research Council.